



# Green synthesis and structural characterization of gold nanoparticles from *Achillea wilhelmsii* leaf infusion and *in vitro* evaluation

MARYAM ASARIHA<sup>1,2</sup>, AZAM CHAHARDOLI<sup>3</sup>, NADIA KARIMI<sup>3</sup>,  
MARYAM GHOLAMHOSSEINPOUR<sup>3</sup>, ALIREZA KHOSHROO<sup>1,3</sup>, HOUSHANG NEMATI<sup>4</sup>,  
YALDA SHOKOOHINIA<sup>3,5</sup> and ALI FATTAHI<sup>1,3,\*</sup> 

<sup>1</sup>Medical Biology Research Center, Health Technology Institute, Kermanshah University of Medical Sciences, Kermanshah 6734667149, Iran

<sup>2</sup>Student Research Committee, School of Pharmacy, Kermanshah University of Medical Sciences, Kermanshah 6734667149, Iran

<sup>3</sup>Pharmaceutical Sciences Research Center, Health Institute, School of Pharmacy, Kermanshah University of Medical Sciences, Kermanshah 6734667149, Iran

<sup>4</sup>Fertility and Infertility Research Center, Health Technology Institute, Kermanshah University of Medical Sciences, Kermanshah 6734667149, Iran

<sup>5</sup>Ric Scalzo Botanical Research Institute, Southwest College of Naturopathic Medicine, Tempe, AZ, USA

\*Author for correspondence (a.fatahi.a@gmail.com)

MS received 2 April 2019; accepted 18 August 2019; published online 29 January 2020

**Abstract.** The aim of this study is to green-synthesize gold nanoparticles (GNPs) by leaf infusion of *Achillea wilhelmsii* (AW) and to evaluate their biological effects. The synthesized AW-GNPs were characterized by UV-Vis spectroscopy, Fourier transform infrared, X-ray diffraction (XRD), transmission electron microscopy (TEM) and dynamic light scattering analyses. The antibacterial and cytotoxicity activities of AW infusion and AW-GNPs were evaluated. Antioxidant activity was evaluated by 1, 1-diphenyl-2-picrylhydrazyl test. Moreover, the electrochemical activity of AW-GNPs as a modifier at a glassy carbon electrode (GCE) was studied. The surface plasmon resonance absorption band at 540 nm in the UV-Vis spectrum discloses the reduction of gold cations into GNPs. The XRD pattern of GNPs shows the crystal structure of AW-GNPs, and TEM image displays the spherical shape of GNPs with small size (2.7–38.7 nm). The AW infusion and AW-GNPs demonstrated a maximum antioxidant activity of 68 and 58%, respectively. AW-GNPs showed antibacterial activity against gram-positive bacteria, without affecting gram-negative bacteria. Also, AW-GNPs exhibited the cytotoxicity effects against MDA-MB-468 cancer cell line, and the electrochemical study indicated a significant electrocatalytic activity of AW-GNPs. The results indicate the advantages of using AW leaf infusion for the production of GNPs with antibacterial, antioxidant, cytotoxic and electrocatalytic activities.

**Keywords.** Green synthesis of gold nanoparticles; *Achillea wilhelmsii*; antimicrobial properties; electrochemical catalysis; antioxidant; cytotoxic effect.

## 1. Introduction

These days, with the enormous progress in nanobiotechnology, gold nanoparticles (GNPs) have been applied in biomedical sciences [1], including biotechnology [2], microbiology [3], oncology, drug delivery [4], tissue/tumour imaging, photothermal therapy [5] and nucleic acid labelling [6]. There are different physical [7] and chemical [8] methods for producing GNPs. However, these methods have several drawbacks, e.g. the instability and agglomeration of nanoparticles, the difficulty in controlling the growth of crystals and the toxicity of chemicals [9,10]. As an alternative, green synthesis of GNPs represents interesting topics and draws more attention to the rapidly growing area of nanotechnology [11].

For the green synthesis of GNPs, numerous plants' extracts have been applied as reducing and stabilizing agents. Among them, the medicinal plants show more advantage because of the synergistic effect of their therapeutic ingredients.

*Achillea wilhelmsii* (AW) is the most essential medicinal plant and belongs to the Asteraceae (Compositae) family; this genus encompasses over 120 species worldwide [12]. AW is widespread all over the world, and its species have been used as a folk or traditional herbal medicine [13]. It is native in Western Asia and Europe, although it is found in North America, Australia, New Zealand [14] and different parts of Iran (with the local name of 'Boomadaran') [15]. Biological activities of AW include anti-hypertensive and anti-hyperlipidemic [16,17],

anti-inflammatory [18,19], anti-tumoural [20], antispasmodic [21], antioxidant [22,23] and antibacterial [24,25], which are relative to its secondary metabolites, e.g. alkaloids (achilleine), flavonoids, cineol, sesquiterpenoids,  $\alpha$ - and  $\beta$ -pinen, camphor, rutin, thujene, caryophyllene, borneol, volatile oils and monoterpenoids [26–28].

Andeani *et al* [29] showed the capacity of AW flower extract for the synthesis of GNP, but their study was limited to physical characterization of particles. In the current study, we introduce a safe, non-toxic and eco-friendly synthesis of GNPs by AW leaf infusion as a reductant and stabilizer. To the best of our knowledge, this is a complete and comprehensive report on the antibacterial, antioxidant, cytotoxic and electrocatalytic properties of GNPs synthesized with AW leaf infusion.

## 2. Experimental

### 2.1 Materials

Chloroauric acid ( $\text{HAuCl}_4$ ), dimethyl sulphoxide (DMSO), 3-(4,5-dimethylthiazol-2-yl)-2,5-diphenyltetrazolium bromide (MTT), 1,1-diphenyl-2-picrylhydrazyl (DPPH), Mueller–Hinton agar and broth, methanol, Folin–Ciocalteu reagent, aluminium chloride ( $\text{AlCl}_3$ ), gallic acid and quercetin were purchased from Sigma-Aldrich, USA. Other analytical grade compounds were used without any further purification and purchased from Merck, Germany. MDA-MB-468,  $\beta$ TC-3 cell lines and all microorganisms, including *Bacillus subtilis* (ATCC 6633), *Staphylococcus epidermidis* (ATCC 12228), *Escherichia coli* (ATCC 25922) and *Salmonella enterica* (ATCC 9270) were purchased from Pasteur institute Cell Bank, Tehran, Iran. Fibroblast as the normal cell was isolated by the procedure described in our previous work [30]. All the cell culture ingredients were supplied from Auto-cell Co., Poland.

### 2.2 Preparation of infusion from AW leaf and synthesis of GNPs

AW leaves were collected in the Islamabad-e Gharb Mountain surrounding Kermanshah (Iran) at an altitude of 1600 m above sea level in May 2017. To avoid variation in composition and concentration of secondary metabolites, leaves were harvested one time and in one day. The plant species was recognized by Dr Nastaran Jalilian, Forests and Rangelands Research Department, Razi University, Kermanshah, Iran. After washing and drying the leaves, dried leaves were milled to produce a fine powder. Then, a 5% suspension was prepared by adding 100 ml of boiling distilled water to 5 g of the powder, and the mixture was stirred at boiling point for 15 min; the mixture was cooled down; the cooled mixture was centrifuged for 20 min at 8000 rpm and filtered with a filter paper (No. 1) to achieve a transparent infusion. In order to synthesize GNPs, the infusion was added to 1 mM

chloroauric acid solution in a ratio of 1:9 (v/v %) and stirred at 60°C. After 5 min, the heat supply was cut off, and the solution was stirred at ambient temperature until a colour change was observed from yellow to dark purple, indicating the formation of AW-GNPs.

### 2.3 Characterization of GNPs

**2.3a UV–Vis spectroscopy analysis:** UV–Vis analysis was carried out using a Specord 210 plus (Analytik Jena, Germany) over the wavelength range of 300–800 nm, and a resolution of 1 nm to confirm the synthesis of GNPs, indirectly. The wavelength range of surface plasmon resonance (SPR) for GNPs is 500–550 nm [31].

**2.3b FT-IR spectroscopy analysis:** The functional groups of the infusion and AW-GNPs were characterized by Fourier transform infrared (FT-IR) spectroscopy. FT-IR analysis was carried out using an IR Prestige-21 Shimadzu Spectrometer, Kyoto, Japan, in the spectral range of 400–4000  $\text{cm}^{-1}$  (resolution of 4  $\text{cm}^{-1}$ ) at room temperature using potassium bromide pellets.

**2.3c XRD analysis:** To confirm the crystalline nature of the synthesized AW-GNPs, X-ray diffraction (XRD) spectrum was recorded using an APD 2000 X-ray generator (Novara, Italy), which worked at 40 kV and 30 mA with Cu K-alpha radiation.

**2.3d Transmission electron microscopy analysis:** Transmission electron microscopy (TEM) has been applied for characterization of the morphology and particle size of AW-GNPs using a LEO 906 microscope (Carl Zeiss, Germany), with 100 kV accelerating voltage. Before analysis, GNPs were deposited on carbon–copper grids.

**2.3e Dynamic light scattering and zeta potential:** The particle size and surface charge of AW-GNPs were measured using a Nano ZS Zetasizer (Malvern Instruments Ltd., Worcestershire, UK) at the wavelength of 632.8 nm and at 25°C. The laser doppler electrophoresis technique was applied to determine the zeta potential of AW-GNPs in water.

### 2.4 Phenolic and flavonoid assays

The contents of phenolic compounds of AW infusion and AW-GNPs were measured by the Folin–Ciocalteu method [32]; 0.25 ml of AW infusions or AW-GNPs suspensions was added to 1.25 ml of Folin–Ciocalteu reagent (0.2 N fresh solution). After 5 min, 1 ml of sodium carbonate (75  $\text{g l}^{-1}$ ) was added to the mixture. After 2 h incubation at ambience, the absorbance of samples at 760 nm was measured. The calibration curve was drawn using gallic acid as a standard, and the total phenolic content calculated *via* this standard curve was expressed as  $\mu\text{g}$  gallic acid equivalent ( $\mu\text{GAE}$ ) per g of dry weight (gDW).

The total flavonoid content was determined by the Quettier-Deleu [33] method with a brief revision. An aluminium chloride solution containing 2% methanol was added to AW infusions of different concentrations and AW-GNPs, and the absorbance was determined at 415 nm. The standard curve of Quercetin was used to measure the total flavonoid content in terms of  $\mu\text{g}$  Quercetin equivalent ( $\mu\text{QE}$ ), shown as  $\mu\text{QE}$  per gDW.

## 2.5 DPPH antioxidant assay

The antioxidant ability of AW infusion and AW-GNPs was anticipated by measuring DPPH activity [34]; 0.5 ml of AW infusion and AW-GNPs at concentrations of 50, 100, 150, 200, 250 and 300  $\mu\text{g ml}^{-1}$  were mixed with 0.5 ml of DPPH solution (0.1 mM solution in methanol), and well-shaken mixtures were stored in dark environment for 30 min. Finally, the absorbance of each mixture was recorded at 517 nm using the UV-Vis spectrophotometer. Absorbance of a mixture of 0.5 ml methanol and 0.5 ml DPPH solution was recorded as a control. Antioxidant activity was determined [4] by the following equation:

$$\begin{aligned} \text{antioxidant activity (\%)} \\ = [(\text{OD control} - \text{OD sample}) / \text{OD control}] \times 100. \quad (1) \end{aligned}$$

## 2.6 MTT assay

The cytotoxicity of AW infusion and AW-GNPs at various concentrations (10, 25, 50, 100, 150  $\mu\text{g ml}^{-1}$ ) was evaluated by MTT assay [35]. MDA-MB-468 (a breast cancer cell line),  $\beta\text{TC-3}$  (a pancreatic cancer cell line) and normal human fibroblast cells were applied in this study; 180  $\mu\text{l}$  of cell suspension at the concentration of 10000 cells per well was seeded on the wells of clear-bottom 96-well tissue culture plates. Dulbecco's Modified Eagle's Medium (DMEM)-F12 supplemented with 10% Fetal Bovine Serum, 50 units  $\text{ml}^{-1}$  Penicillin and 50  $\mu\text{g ml}^{-1}$  Streptomycin was used as a medium. Plates were incubated in a  $\text{CO}_2$  incubator (37°C, 5%  $\text{CO}_2$ , 95% humidity) for 24 h; later, 20  $\mu\text{l}$  of treatment solutions at different concentrations was added into each well, and the plates were incubated for further 48 h. Cells were then incubated with fresh medium containing 0.5  $\text{mg ml}^{-1}$  MTT for 4 h. Finally, wells were washed with PBS; 150  $\mu\text{l}$  of DMSO was added to each well to dissolve the formazan crystal, and ultimately, the absorbance was measured at 540 and 630 nm using an ELISA plate reader (Synergy H1, Biotek, USA). Percentage of cell viability was calculated by the following equation:

$$\begin{aligned} \text{cell viability (\%)} = (A_{540} - A_{630})_S / (A_{540} - A_{630})_C \\ \times 100 \quad (2) \end{aligned}$$

where  $(A)_S$  is the optical absorbance of the samples and  $(A)_C$  is the optical absorbance of the standard samples.

## 2.7 Antimicrobial activities

To compare green synthesis to chemical one in the antibacterial study, chemical gold nanoparticles (ChGNPs) synthesized by citrate reduction method were used [36]. For evaluating the antibacterial effects of AW infusion, ChGNPs and AW-GNPs, the CLSI-M07-A8 method was applied. Total counts of isolated strains of gram-negative (*E. coli* and *S. enterica*) and gram-positive (*S. epidermidis* and *B. subtilis*) bacteria were standardized to equivalent at  $1 \times 10^8$  CFU  $\text{ml}^{-1}$  (0.5 Mac Farland standard) using Mueller-Hinton broth. Agar well diffusion method and the broth dilution susceptibility assay were applied to study antibacterial activity.

**2.7a Well diffusion assay:** To measure the antibacterial effects of AW infusion and AW-GNPs on gram-negative and gram-positive bacteria by the well-diffusion method,  $1 \times 10^8$  CFU  $\text{ml}^{-1}$  of bacteria suspensions was inoculated onto Mueller-Hinton agar plates; 100  $\mu\text{l}$  of AW infusion or AW-GNPs (at concentrations of 16.75, 33.5, 75, 150 and 300  $\mu\text{g ml}^{-1}$ ) was added into the 6 mm diameter wells; after incubation of the plates at 37°C for 24 h, the inhibition zone was calculated using a ruler.

**2.7b Minimum inhibitory concentration:** Bacterial cells were cultured into 96-well plates at the final concentration of  $1 \times 10^8$  CFU  $\text{ml}^{-1}$ . Later 50  $\mu\text{l}$  of AW infusion or AW-GNPs at concentrations of 16.75, 33.5, 75, 150 and 300  $\mu\text{g ml}^{-1}$  was added to wells as the serial solution, and after 24 h at 37°C, the cell number was counted; the positive and negative controls were the bacteria-inoculated medium and pure medium, respectively. The minimum inhibitory concentration (MIC) was calculated based on the lowest concentration of AW infusion or AW-GNPs that is necessary for the inhibition of the bacterial growth. If there was no bacterial growth after inoculation in plate agar, that was taken as the minimum bactericidal concentration (MBC) [37].

## 2.8 Electrochemical measurement procedure

Electrochemical experiments were performed using an Autolab PGSTAT101 potentiostat/galvanostat (Eco Chemie, Netherlands) controlled by NOVA Auto-Lab software. An Ag/AgCl/KCl (3.0 M) as a reference electrode, a platinum wire as a counter-electrode and a glassy carbon electrode (GCE) or a modified GCE with GNPs as the working electrode in a conventional three-electrode cell were used, and all experiments were performed at ambient temperature.

To prepare the modified GCE, the GCE was polished with emery paper followed by alumina (1 and 0.05  $\mu\text{m}$ ) and then washed with distilled water; 10  $\mu\text{l}$  of AuNPs suspension (1  $\text{mg ml}^{-1}$ ) was cast on the surface of GCE, and the solvent was let to evaporate at room temperature. The electrocatalytic activity of AW-GNPs for 1.0 mM ascorbic acid (AA) and 1.0 mM dopamine (DA) oxidation was characterized by cyclic voltammetry (CV) in PBS (0.1 M, pH 7.4) [38].

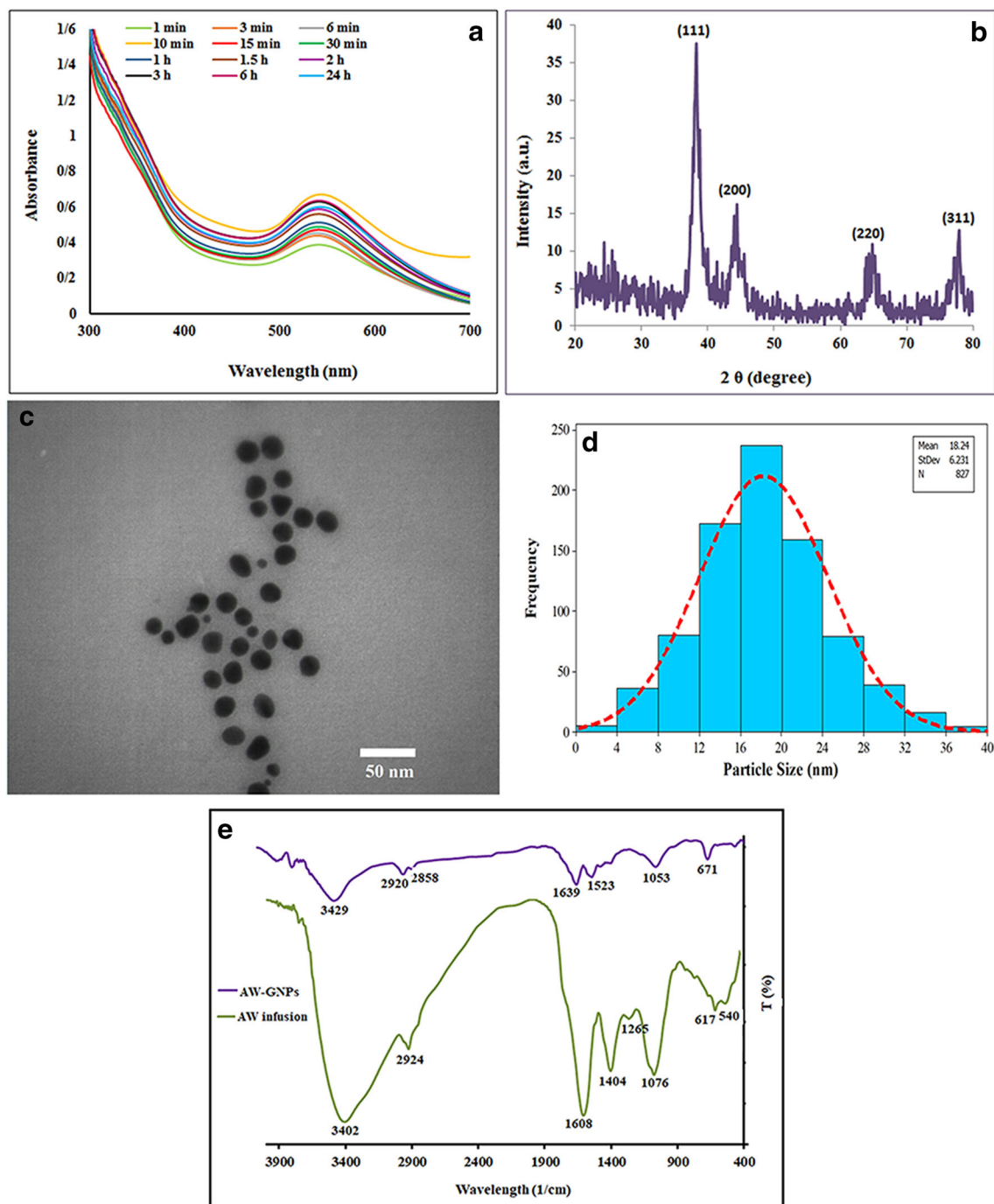


**Figure 1.** (a) UV–Vis spectra of GNPs biosynthesized by AW infusion, (b) XRD spectrum of AW-GNPs, (c) TEM image of AW-GNPs, (d) particle size distribution of AW-GNPs and (e) FT-IR spectrum of AW infusion and AW-GNPs.

### 3. Results and discussion

#### 3.1 Characterization of AW-GNPs

UV–Vis spectroscopy is a useful technique to detect formation, crystal growth, size and stability of GNPs [13]. The reduction of the  $\text{HAuCl}_4$  solution in the presence of AW leaf infusion was monitored at different time intervals

(figure 1a). The maximum absorption determined by UV–Vis spectrophotometric analysis was 540 nm. In this procedure, the temperature of  $60^\circ\text{C}$  was maintained for 5 min and after this, the heat supply was cut off. The high temperature speeded up the synthesis of AW-GNPs, which could decrease the size of nanoparticles and create spherical particles. The colour change was observed 1 min after the mixing of the infusion and the  $\text{HAuCl}_4$  solution, which proved the formation of

AW-GNPs by the reduction of  $\text{Au}^{3+}$  ions to  $\text{Au}^0$ . During the 5 min of the reaction time, the colour of the sample changed from yellowish to dark purple. The intensity of  $\lambda_{\text{max}}$  increased during the time from 1 to 10 min, indicating that the concentration of AW-GNPs had increased. After 10 min, no significant enhancement and shift in  $\lambda_{\text{max}}$  were observed until 24 h, indicating that the reaction was finished after 10 min, and nanoparticles were stable during the time.

The FT-IR spectra of AW infusion and AW-GNPs are shown in figure 1e. FT-IR reveals the functional groups of the possible biomolecules responsible for bioreduction of  $\text{HAuCl}_4$ , capping and stabilization of AW-GNPs. As shown in the FT-IR spectrum (figure 1e), the main peaks of AW infusion are at  $3402\text{ cm}^{-1}$  (feature of the broad peak of O–H group or N–H stretching vibration of amine),  $2924\text{ cm}^{-1}$  (characteristic of C–H stretching vibration of aliphatic),  $1608\text{ cm}^{-1}$  (feature of N–H bending vibration of primary amine),  $1404\text{ cm}^{-1}$  (C–H stretching bending of  $\text{CH}_3$ ) and  $1265$  and  $1060\text{ cm}^{-1}$  (characteristic of C–O stretching vibration). O–H and N–H groups are the main functional groups present in the alkaloids, phenolic compounds, flavonoids and proteins. The FT-IR spectrum of AW-GNPs (figure 1e) shows peaks at  $3429$  and  $1639\text{ cm}^{-1}$ , which are, respectively, characteristics of N–H stretching and bending vibration of primary and secondary amines or amides. There are peaks at  $2920$  and  $2858\text{ cm}^{-1}$  (characteristics of the C–H stretching vibration of alkanes), and two peaks at  $1523$  and  $1458\text{ cm}^{-1}$  (characteristic of the C=C stretching vibrations of the benzyl). The peak at  $1053\text{ cm}^{-1}$  is a characteristic of the C–O stretching vibrations. These results confirmed the presence of AW infusion compounds in the spectrum of AW-GNPs, although the intensity of peaks in the spectrum of AW infusion was higher than that of AW-GNPs. The presence of N–H and aliphatic C–H in the spectra is the sign for the presence of proteins on the surface of AW-GNPs; this protein corona can prevent the agglomeration of NPs [39].

The XRD analysis shows the purity and crystal structure of the synthesized nanoparticles. Figure 1b shows the XRD pattern of the synthesized AW-GNPs from AW infusion, which reveals four well-defined characteristic peaks in the  $2\theta$  range ( $20$ – $80^\circ$ ). The diffraction peaks of AW-GNPs are detected at  $37.8$ ,  $44.6$ ,  $64.6$  and  $77.5^\circ$ , which correspond to (111), (200), (220) and (311) crystalline planes, respectively. This presents a reflection of the face-centre cubic structure of AW-GNPs, signalling that the synthesized GNP is composed of a crystalline structure. The Debye–Scherrer equation [40] was used for estimation of the average crystallite size of synthesized GNPs as follows.

Scherrer equation:

$$S = \frac{k\lambda}{\beta \cos \theta} \quad (3)$$

where  $S$  is the crystal size of GNPs,  $\lambda$  is the wavelength of the X-ray source ( $1.54056\text{ \AA}$ ) used in the XRD,  $\beta$  is the full-width at half-maximum of the (111) diffraction peak in radians,

$k$  is the Scherrer constant, which varies in the range of  $0.9$ – $1$  (taken as  $0.9$ ) and  $\theta$  is the Bragg angle in radians. The size of the synthesized GNPs was estimated at around  $9.4\text{ nm}$ .

AW-GNPs were also characterized by TEM. AW-GNPs were mostly spherical with a few traces of triangular, square and pentagonal particles (figure 1c). The particle size of AW-GNPs was in the range of  $2.7$ – $38.7\text{ nm}$  (figure 1d).

The results of the dynamic light scattering (DLS) analysis showed that the average hydrodynamic diameter of AW-GNPs was  $97.82 \pm 2.64\text{ nm}$ . Nanoparticle size distribution could be expressed through the polydispersity index (PDI) value. PDI of AW-GNPs is  $0.307 \pm 0.04$ , which indicates that the system is moderately polydisperse [41,42]. The size of nanoparticles by DLS is different compared with the TEM measurement, because of their different working principles. It is also a well-known fact that DLS measures the thickness of bio-compounds present on the surface of nanoparticles [43]. Therefore, there is a difference between DLS results and TEM [44]. The zeta potential reveals the information about the surface charge of AW-GNPs. The zeta potential of AW-GNPs was  $-27.3 \pm 5.67\text{ mV}$ , which confirmed the reasonable stability of the biosynthesized GNPs.

### 3.2 Content of flavonoid and phenolic compounds

The antioxidant effects and strong reducing activity of phenolic and flavonoid compounds, which are abundant in the plant extracts, are the reason for metal ions reduction and formation of the corresponding metal nanoparticles. Therefore, we quantitatively analysed the total phenolic compounds content in AW-GNPs and AW infusion samples. As can be seen from figure 2a at various concentrations ( $50$ ,  $100$ ,  $150$ ,  $200$ ,  $250$  and  $300\text{ }\mu\text{g ml}^{-1}$ ), the content of total phenolic compounds of synthesized AW-GNPs was  $1037\text{ }\mu\text{GAE per gDW}$ , while it was  $1393\text{ }\mu\text{GAE per gDW}$  for AW infusion.

Determination of the total flavonoid content of AW-GNPs and AW infusion samples was done at different concentrations ( $50$ ,  $100$ ,  $150$ ,  $200$ ,  $250$  and  $300\text{ }\mu\text{g ml}^{-1}$ ; figure 2b). In our study,  $653\text{ }\mu\text{QE per gDW}$  of flavonoid content was observed in the AW-GNPs while  $707\text{ }\mu\text{QE per gDW}$  of flavonoid content was obtained for AW infusion. These results indicated that  $92.36\%$  of flavonoids in infusion were absorbed on the surface of GNPs while  $74.44\%$  of phenolic compounds were present on the surface of NPs.

### 3.3 Antioxidant properties

DPPH assay reveals that the leaf infusion and AW-GNPs are free radical scavengers, which have significant antioxidant property. As can be observed in figure 2c, with increasing concentration, the antioxidant activity of the AW infusions and AW-GNPs increases. The AW-GNPs and AW leaf-infusion showed  $58$  and  $68\%$  of the scavenging effect at a concentration of  $300\text{ }\mu\text{g ml}^{-1}$ , respectively. The AW leaf infusion exhibited a better scavenging activity for DPPH than AW-GNPs, which might be due to the presence of more antioxidant

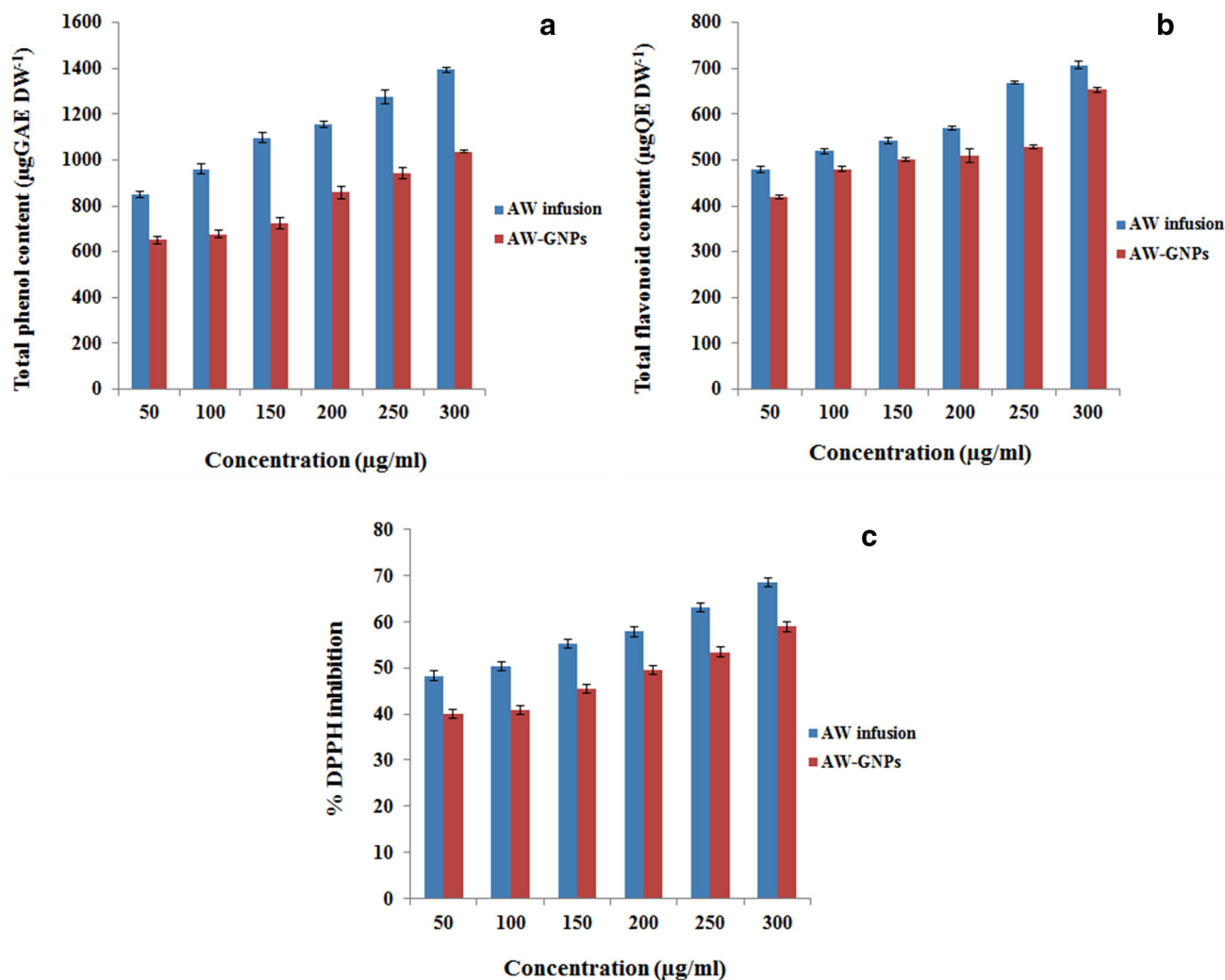


**Figure 2.** (a) Total phenolic content of AW infusion and AW-GNPs at various concentrations ( $\mu\text{GAE}$  per  $\text{gDW}$ ), (b) total flavonoid content of AW infusion and AW-GNPs at various concentrations ( $\mu\text{QE}$  per  $\text{gDW}$ ) and (c) DPPH scavenging activity of AW infusion and AW-GNPs at various concentrations.

compounds in the infusion than in AW-GNPs [44]. The phenolic and flavonoid content of infusion and AW-GNPs confirmed this result; the number of phenolic compounds and flavonoids on the surface of nanoparticles was lower than that of AW infusion [45–47].

### 3.4 Cytotoxicity

The cytotoxicity of AW infusion and AW-GNPs against MDA-MB-468,  $\beta\text{TC-3}$  and normal human fibroblast was obtained by MTT assay. The treatment of cells was carried out with AW infusion and AW-GNPs at different concentrations ( $10\text{--}150 \mu\text{g ml}^{-1}$ ) for 48 h. Based on figure 3a, MDA-MB-468 cell presented high sensitivity to AW infusion and AW-GNPs.

A direct dose–response was observed from the results, and the activity of AW-GNPs was larger than that of the AW

infusion. The small size of these NPs together with organic moieties present in the corona of NPs lets them be easily absorbed on the cell membrane and to be up-taken consequently [48]. Other studies have shown that the particle size and zeta potential of nanoparticles affect their interaction with biological components, e.g. cell membrane, proteins and glycosaminoglycans [49,50].

From figure 3b, when the concentrations of AW infusion and AW-GNPs are increased, the cell viability of human fibroblast decreases slightly. As can be seen from figure 3c, none of the concentrations has a significant effect on  $\beta\text{TC-3}$  cell line. A comparison between MDA-MB-468 and normal human fibroblast cells indicated that AW infusion and AW-GNPs were effective just on MDA-MB-468 cells, and they were not effective on normal fibroblast cells. These results indicated that our synthesized nanoparticles can probably annihilate cancer cells without destroying normal cells.

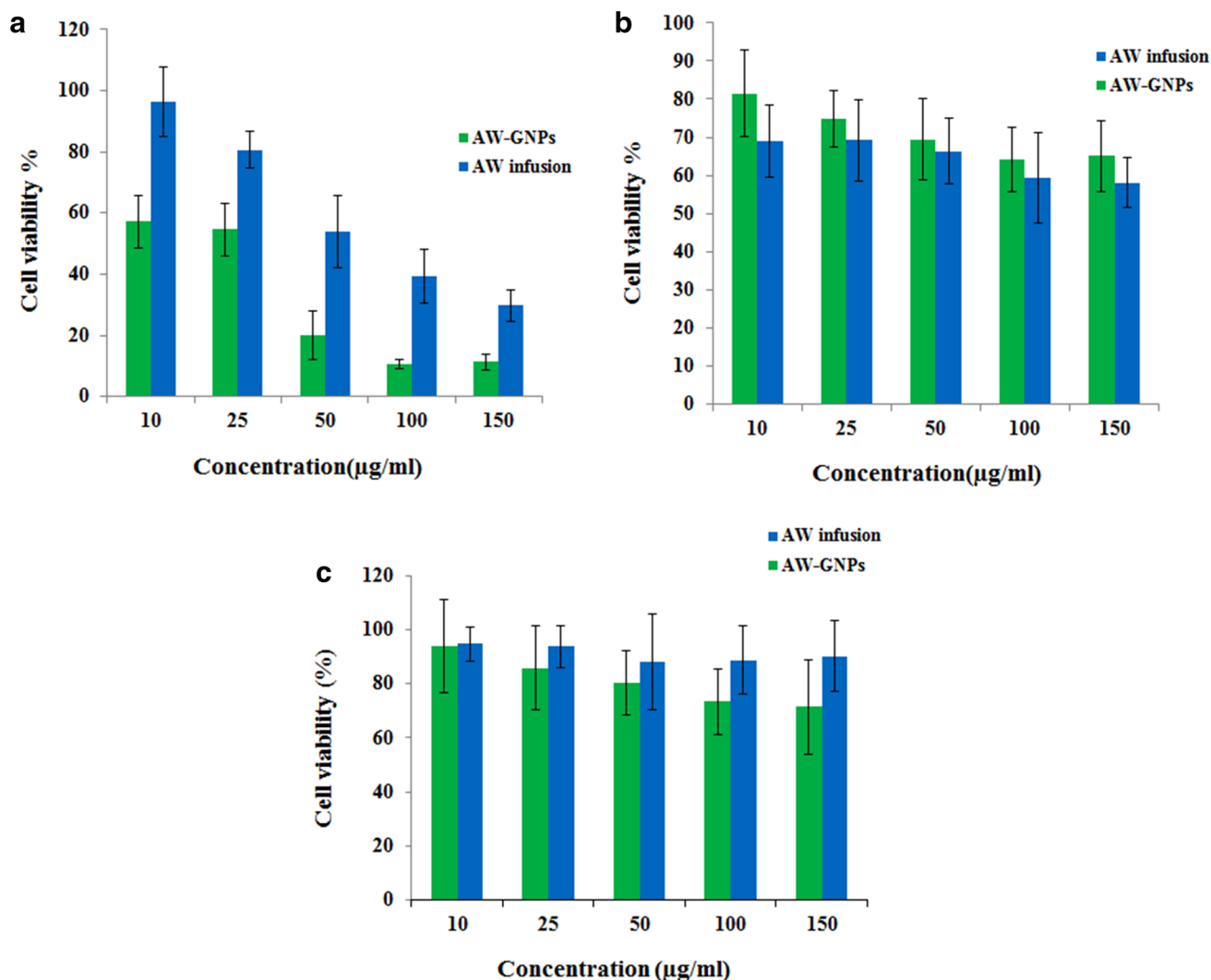


**Figure 3.** *In vitro* cytotoxic of AW infusion and AW-GNPs against: (a) MDA-MB-468, (b) human fibroblast and (c)  $\beta$ TC-3 at various concentrations after 48h. Water was used as a control, and the cell viability of control was taken as the reference (100%). Significance was calculated by ANOVA ( $*p \leq 0.5$ ).

It can also be concluded that AW-GNPs do not affect  $\beta$ TC-3 cells because of the resistance of pancreatic cancerous cells to chemotherapy in comparison with other cancerous cells [51]. As a result, this occurrence indicates that these nanoparticles have different effects on different cancer cells and normal cells.

This difference between normal cells and cancer cells can be related to the presence of different receptors on cancer and normal cells membranes as well as their different functional mechanisms. According to Shahani *et al* [52], *Achillea millefolium* extract had no effect on normal human fibroblast cells. They explained that *A. millefolium* probably has different mechanisms for antiproliferation on normal and cancerous cells. The effect of *Achillea* on cancer cell lines can also be due to its secondary metabolites. It has been shown

that phenolic compounds, flavonoids and antioxidants in the volatile oil of *Achillea* species play a role in cancer inhibition as well as its anti-inflammatory effect [53]. Recently, several studies showed that extracts of *Achillea* species inhibited breast, colon and liver cancers [54,55]. The cytotoxicity study of *Achillea santolina* and *Raphanus sativus* extracts on MCF7 (human breast carcinoma), Caco2 (epithelial colorectal adenocarcinoma) and HepG2 (human hepatocarcinoma) together with normal cell line of WISH (derived from normal amnion) shows that treatment of cancer cell lines with *A. santolina* and *R. sativus* extracts induces cell cycle arrest at G0/G1 phase while normal cell line (WISH) is accumulated in G2/M [56]. Therefore, natural products on the corona of AW-GNs can probably behave differently in normal and cancer cells and can activate different internal pathways in these cells.

**Table 1.** Inhibition zone of AW, ChGNPs and AW-GNPs for bacteria strains.

Bacteria strains	<i>S. epidermidis</i>			<i>B. subtilis</i>			<i>E. coli</i>			<i>S. enterica</i>		
	AW	ChGNPs	AW-GNPs	AW	ChGNPs	AW-GNPs	AW	ChGNPs	AW-GNPs	AW	ChGNPs	AW-GNPs
Extract concentrations ( $\mu\text{g ml}^{-1}$ )												
18.75	—	—	—	—	—	—	—	—	—	—	—	—
37.5	—	—	—	—	—	—	—	—	—	—	—	—
75	—	—	—	—	—	$9 \pm 0.36$	—	—	—	—	—	—
150	—	—	$8 \pm 0.95$	—	—	$10 \pm 0.45$	—	—	—	—	—	—
300	—	—	$10 \pm 0.25$	—	$9 \pm 0.55$	$11 \pm 0.84$	—	—	—	—	—	—
Control (+)		$16.5 \pm 0.96$			$17.5 \pm 0.85$			$26 \pm 0.80$			$24.5 \pm 1$	

**Table 2.** Antibacterial activity of AW and AW-GNPs infusion on gram-positive and gram-negative bacteria.

Bacteria	AW		AW-GNPs	
	MIC ( $\mu\text{g ml}^{-1}$ )	MBC ( $\mu\text{g ml}^{-1}$ )	MIC ( $\mu\text{g ml}^{-1}$ )	MBC ( $\mu\text{g ml}^{-1}$ )
Gram-positive				
<i>B. subtilis</i>	—	—	75	150
<i>S. epidermidis</i>	—	—	150	300
Gram-negative				
<i>E. coli</i>	—	—	—	—
<i>S. enterica</i>	—	—	—	—

MIC: minimum inhibitory concentration, MBC: minimum bactericidal concentration.

### 3.5 Antimicrobial activities

The antibacterial activities of the AW extract, ChGNPs and AW-GNPs were determined against gram-positive and gram-negative bacteria using well diffusion assay. After inoculation in plate agar, the diameter of the inhibition zone was measured. As shown in table 1, the AW-GNPs affect only the *B. subtilis* and *S. epidermidis* bacteria strains at a concentration of 150 and  $300 \mu\text{g ml}^{-1}$ . On the other hand, ChGNPs exhibited antibacterial activity against only *B. subtilis* at the maximum concentration of  $300 \mu\text{g ml}^{-1}$ .

MIC and MBC of AW infusions and AW-GNPs are presented in table 2. As can be seen from table 2, AW-GNPs exhibited antimicrobial properties against gram-positive bacteria, without affecting gram-negative bacteria. In addition, AW infusion did not have antibacterial activity against bacterial strains (gram-positive and gram-negative), at the concentrations used. Some factors are effective on the different responses of bacteria strains; the factors like variance in the construction of the bacterial cell wall and phytochemical composition of the infusion (e.g. flavonoids, tannins, phenols, terpenoids) are effective. Also, the kind of metal ions, shape, size and surface area of nanoparticles are important [57,58].

Interaction of AW-GNPs with the outer membrane of bacteria can change the structure of the membrane, cause degradation of the cell membrane and finally cell death. Therefore, the differences in composition and structure of bacterial cell wall are effective. Due to the thickness of the peptidoglycan layer of gram-positive bacteria, the inhibitory effect of AW-GNPs is probably due to the interaction of the infusion with the cell wall proteins of the bacteria. At these concentrations, the ChGNPs and AW extract did not affect bacteria strains (except for  $300 \mu\text{l ml}^{-1}$  of ChGNPs on *B. subtilis*), but the composition of AW-GNPs has an antibacterial effect. This is probably due to the synergistic effect of AW extract and GNPs at these concentrations, which can attach to the bacterial cell wall and inhibit bacterial growth.

### 3.6 Electrochemical analysis of AW-GNPs

The electrochemical activity of AW-GNPs was studied using CV towards oxidation of AA and DA to evaluate the performance of AW-GNPs. Figure 4 displays the electrochemical oxidation of 1.0 mM AA (figure 4a) and 1.0 mM DA (figure 4b) at bare GCE and GCE modified with AW-GNPs (AW-GNPs-GCE) in 0.1 M PBS (pH 7.4; the scan rate of

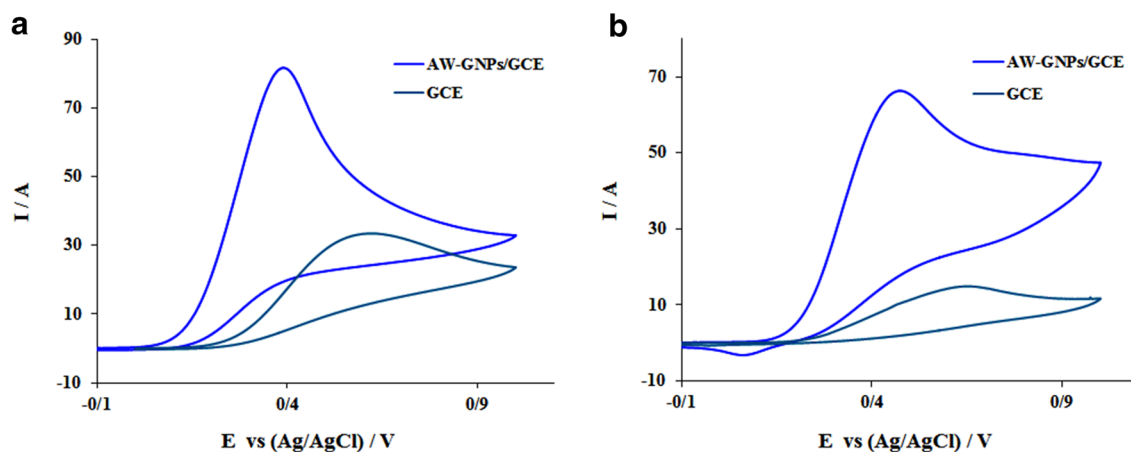


**Figure 4.** (a) Cyclic voltammogram of bare GCE and AW-GNPs–GCE in 0.1 M PBS (pH = 7.4) containing 1.0 mM AA and (b) DA at a scan rate of  $100 \text{ mV s}^{-1}$ .

$100 \text{ mV s}^{-1}$ ). The AW-GNPs–GCE exhibits significantly enhanced electrocatalytic activity *via* the enhancement in peak currents and shift of the peak potentials towards less positive potential for the oxidation of AA and DA, compared with bare GCE. As can be seen, the peak potentials for AA and DA oxidation at the bare electrode are about 610 and 650 mV, while the corresponding peak potentials at AW-GNPs–GCE are 400 and 470 mV, respectively. Also, the oxidation peak currents of AA and DA on AW-GNPs–GCE were improved considerably.

#### 4. Conclusion

In the present work, GNPs were synthesized with AW leaf infusion by means of stabilizing and reducing agents. This is a facile, eco-friendly process and has potent applications in pharmaceuticals and biomedicine. GNPs were well characterized by UV–Vis spectroscopy, and further characterization was done using FT-IR spectroscopy, XRD, TEM and DLS analyses. The antioxidant properties of AW infusion and AW-GNPs were proved by DPPH radical scavenging. The synthesized GNPs showed efficient antimicrobial activities against *B. subtilis* and *S. epidermidis* (gram-positive bacteria). The cytotoxicity activities of AW infusion and AW-GNPs were determined on MDA-MB-468,  $\beta$ TC-3 and human fibroblast cells. The MDA-MB-468 cell line was more sensitive than others. Also, the electrochemical studies of GNPs synthesis from AW infusion indicate their application in the fabrication of sensors and biosensors in electrochemistry field.

#### Acknowledgements

The authors gratefully acknowledge the Research Council of Kermanshah University of Medical Sciences for financial support. This work was performed in partial fulfilment

of the requirements for MS of Maryam Asariha, School of Pharmacy, Kermanshah University of Medical Sciences, Kermanshah, Iran.

#### References

- [1] Rajeshkumar S 2016 *J. Genet. Eng. Biotechnol.* **14** 195
- [2] Aromal S A and Philip D 2012 *Spectrochim. Acta A* **97** 1
- [3] Dorosti N and Jamshidi F 2016 *J. Appl. Biomed.* **14** 235
- [4] Ghosh P, Han G, De M, Kim C K and Rotello V M 2008 *Adv. Drug Deliv. Rev.* **60** 1307
- [5] Gui C and Cui D X 2012 *Cancer Biol. Med.* **9** 221
- [6] Tang D, Yuan R and Chai Y 2006 *Biotechnol. Bioeng.* **94** 996
- [7] Mafuné F, Kohno J Y, Takeda Y and Kondow T 2002 *J. Phys. Chem. B* **106** 7575
- [8] Sun Y and Xia Y 2002 *Science* **298** 2176
- [9] Huang H and Yang X 2005 *Colloids Surf. A* **255** 11
- [10] Mandal D, Bolander M E, Mukhopadhyay D, Sarkar G and Mukherjee P 2006 *Appl. Microbiol. Biotechnol.* **69** 485
- [11] Kim J, Rheem Y, Yoo B, Chong Y, Bozhilov K N, Kim D *et al* 2010 *Acta Biomater.* **6** 2681
- [12] Dokhani S, Cottrell T, Khajeddin J and Mazza G 2005 *Plant Foods Hum. Nutr.* **60** 55
- [13] Mahmoudabady M, Lashkari M, Niazmand S and Soukhtanloo M 2017 *J. Tradit. Complement. Med.* **7** 501
- [14] Ali N, Shah S W A, Shah I, Ahmed G, Ghias M and Khan I 2011 *BMC Complement. Altern. Med.* **11** 106
- [15] Alfatemi S M H, Rad J S, Rad M S, Mohsenzadeh S and da Silva J A T 2015 *Biotech.* **5** 39
- [16] Niazmand S, Esparham M, Rezaee S and Harandizadeh F 2011 *Avicenna J. Phytomed.* **1** 51
- [17] Asgary S, Naderi G, Sarrafzadegan N, Mohammadifard N, Mostafavi S and Vakili R 2000 *Drugs Exp. Clin. Res.* **26** 89
- [18] Benedek B, Kopp B and Melzig M F 2007 *J. Ethnopharmacol.* **113** 312
- [19] Benedek B, Rothwangl-Wiltschnigg K, Rozema E, Gjoncaj N, Reznicek G, Jurenitsch J *et al* 2008 *Int. J. Pharm. Sci.* **63** 23
- [20] Csupor-Löffler B, Hajdú Z, Zupkó I, Réthy B, Falkay G, Forgo P *et al* 2009 *Phytother. Res.* **23** 672

- [21] Yaeesh S, Jamal Q, Khan A U and Gilani A H 2006 *Phytother. Res.* **20** 546
- [22] Fathi H, Aghaee L and Ebrahimzadeh M 2011 *Pharmacology-online* **2** 942
- [23] Nemeth E and Bernath J 2008 *Curr. Pharm. Des.* **14** 3151
- [24] Stojanović G, Radulović N, Hashimoto T and Palić R 2005 *J. Ethnopharmacol.* **101** 185
- [25] Mahady G B, Pendland S L, Stoia A, Hamill F A, Fabricant D, Dietz B M *et al* 2005 *Phytother. Res.* **19** 988
- [26] Hosseini M, Harandizadeh F, Niazmand S, Soukhtanloo M and Mahmoudabady M 2013 *Indian J. Physiol. Pharmacol.* **57** 418
- [27] Niazmand S and Khoshnood E 2011 *Iran. J. Basic Med. Sci.* **14** 151
- [28] Javidnia K, Miri R and Sadeghpour H 2004 *DARU J. Pharm. Sci.* **12** 63
- [29] Andeani J K, Kazemi H, Mohsenzadeh S and Safavi A 2011 *Dig. J. Nanomater. Bios.* **6** 1011
- [30] Safdari M, Shakiba E, Kiaie S H and Fattahi A 2016 *Fibers Polym.* **17** 744
- [31] Shankar S S, Rai A, Ahmad A and Sastry M 2004 *J. Colloid Interface Sci.* **275** 496
- [32] Blainski A, Lopes G C and De Mello J C P 2013 *Molecules* **18** 6852
- [33] Quettier-Deleu C, Gressier B, Vasseur J, Dine T, Brunet C, Luyckx M *et al* 2000 *J. Ethnopharmacol.* **72** 35
- [34] Choi C W, Kim S C, Hwang S S, Choi B K, Ahn H J, Lee M Y *et al* 2002 *Plant Sci.* **163** 1161
- [35] van Meerloo J, Kaspers G J and Cloos J 2011 *Cancer cell culture: methods and protocols* (Berlin: Springer) p 237
- [36] Nemati H, Ghahramani M H, Faridi-Majidi R, Izadi B, Bahrami G, Madani S H *et al* 2017 *J. Control. Release* **28** 259
- [37] Chahardoli A, Karimi N and Fattahi A 2018 *Adv. Powder Technol.* **29** 202
- [38] Paimard G, Gholivand M B and Shamsipur M 2016 *Measurement* **77** 269
- [39] Ajitha B, Reddy Y A K and Reddy P S 2014 *Spectrochim. Acta A* **121** 164
- [40] Raman M and Doble M 2014 *J. Appl. Phycol.* **26** 2183
- [41] Lee J, Kim H Y, Zhou H, Hwang S, Koh K, Han D W *et al* 2011 *J. Mater. Chem.* **21** 13316
- [42] Bhattacharjee S 2016 *J. Control. Release* **235** 337
- [43] Adavallan K and Krishnakumar N 2014 *Adv. Nat. Sci. Nanosci.* **5** 025018
- [44] Ahmad T, Bustam M A, Irfan M, Moniruzzaman M, Asghar H M A and Bhattacharjee S 2018 *J. Mol. Struct.* **1159** 167
- [45] Nakkala J R, Bhagat E, Suchiang K and Sadras S R 2015 *J. Mater. Sci. Technol.* **31** 986
- [46] Nakkala J R, Mata R and Sadras S R 2016 *Process Saf. Environ. Prot.* **100** 288
- [47] Kuppusamy P, Yusoff M M, Ichwan S J, Parine N R, Maniam G P and Govindan N 2015 *J. Ind. Eng. Chem.* **27** 59
- [48] Lee K, Nagajyothi P, Sreekanth T and Park S 2015 *J. Ind. Eng. Chem.* **26** 67
- [49] Chahardoli A, Karimi N, Sadeghi F and Fattahi A 2018 *Artif. Cells Nanomed. Biotechnol.* **46** 579
- [50] Park M V, Neigh A M, Vermeulen J P, de la Fonteyne L J, Verharen H W, Briedé J J *et al* 2011 *Biomaterials* **32** 9810
- [51] Amanam I and Chung V 2018 *Cancers* **10** 36
- [52] Shahani S, Hamzkanlu N, Zakeri N and Hosseinimehr S 2015 *Res. Mol. Med.* **3** 10
- [53] Abd-Alla H I, Shalaby N M, Hamed M A, El-Rigal N S, Al-Ghamdi S N and Bouajila J 2016 *Arch. Pharm. Res.* **39** 10
- [54] Choucry M A 2017 *J. Pharmacogn. Phytother.* **9** 1
- [55] El-sharkawy E R 2014 *Chem. Mater. Res.* **6** 85
- [56] Salem M L, Gaafar R M, Mohasseb R N and Abd-Elbaseer M A 2018 *J. Cancer Biomed. Res.* **1** 24
- [57] Balakumaran M, Ramachandran R, Balashanmugam P, Mukeshkumar D and Kalaichelvan P 2016 *Microbiol. Res.* **182** 8
- [58] Srivastava N and Mukhopadhyay M 2015 *J. Clust. Sci.* **26** 675